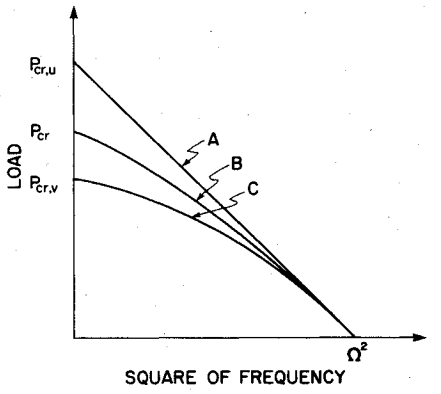

Fig. 1 Eigencurves: A) Rayleigh line; B) eigencurve of the nonconservative system; C) eigencurve of the corresponding conservative system.

The exact critical load of the corresponding conservative system is

$$\bar{P}_{cr} = \frac{-\int_0^\ell K(v_1)v_1 dx}{p_c \int_0^\ell F_c(v_1)v_1 dx} \tag{16}$$

Let us now obtain an approximate critical load for the nonconservative system, using the fundamental buckling mode of the corresponding conservative system as the approximate deflection function, i.e.,

$$y(x) = v_1(x) \tag{17}$$

Using Galerkin's method, we get:

$$P_{cr,v} = \frac{-\int_0^\ell K(v_1)v_1 dx}{p_c \int_0^\ell F_c(v_1)v_1 dx + p_n \int_0^\ell F_n(v_1)v_1 dx} \tag{18}$$

The second term in the denominator is zero, because of Eq. (4). Comparison of Eqs. (16) and (18) yields,

$$P_{cr,v} = \bar{P}_{cr} \tag{19}$$

Leipholz and Huseyin[3] have shown that the critical load of the corresponding conservative system is a lower bound to the critical load of the preceding divergence-type nonconservative system, i.e.,

$$P_{cr} \geq \bar{P}_{cr} \tag{20}$$

From Eqs. (19) and (20),

$$P_{cr} \geq P_{cr,v} \tag{21}$$

Equations (12) and (21) may be summarized by the following Theorem: the approximate critical load of an undamped, one-dimensional, divergence-type nonconservative elastic system, in which the work done by the nonconservative component of the external forces is zero, is an upper bound, if the deflection of the system is approximated by the fundamental vibration mode of the corresponding free system; it is a lower bound if the deflection of the system is approximated by the fundamental buckling mode of the corresponding conservative system.

References

[1] Bolotin, V. V., *Nonconservative Problems of the Theory of Elastic Stability*, Pergamon Press, New York, 1963.

[2] Leipholz, H. H. E. and Huseyin, K., "On the Stability of One-Dimensional Continuous Systems with Polygenic Forces," *Meccanica*, Vol. 6, 1971, pp. 253-257.

[3] Huseyin, K. and Leipholz, H. H. E., "Divergence Instability of Multiple-Parameter Circulatory Systems," *Quarterly of Applied Mathematics*, Vol. 31, 1973, pp. 185-197.

[4] Leipholz, H. H. E., "On Certain Nonconservative Elastic Systems Having Divergence Buckling Loads," *Mechanics Research Communications*, Vol. 1, 1974, pp. 245-249.

[5] Leipholz, H. H. E., "Anwendung des Galerkinschen Verfahrens auf nichtkonservative Stabilitats probleme des elastichen Stabes," *Zeitschrift fur Angewandte Mathematik und Physik*, Vol. 13, 1962, pp. 359-372.

[6] Leipholz, H. H. E., "Uber die Konvergenz des Galerkinschen Verfahrens bei nichtselbstadjungierten und nichtkonservativen Eigenvert problemen," *Zeitsehrift fur Angewandte Mathematik und Physik*, Vol. 14, 1963, pp. 70-79.

[7] Leipholz, H. H. E., "Uber die Zulassigkeit des Verfahren von Galerkin bei linearen, nichtselbstadjungierten Eigenvert problemen," *Zeitschrift fur Angewandte Mathematik und Physik*, Vol. 16, 1965, pp. 837-843.

Experimental Investigation of Underexpanded Exhaust Plumes

Jean-Claude Lengrand,* Jean Allègre,† and Michel Raffin†
Laboratoire d'Aérothermique du Centre National de la Recherche Scientifique, Meudon, France

In a recent paper,[1] one of the authors presented an approximate model for calculating highly underexpanded rocket exhaust plumes. The aim of the present work is to compare original experimental results with the predictions of the reported model.

Calculations

Our calculations are based on the following assumptions:

1) The flowfield is divided into two regions separated by a thin viscous layer: the external atmosphere and an inner region, where the exhaust gas is unaffected by the external atmosphere, and thus behaves as in a vacuum expansion.[2]

2) Within the inner region, the streamlines are radial, the local velocity U is equal to its limiting value U_L, and the evolution is isentropic along the streamlines. The exhaust gas is assumed to be perfect with constant specific heat ratio γ. Considering polar coordinates R, θ centered on the source, the continuity equation yields

$$(\rho U_L)/(\rho_e U_e) = A f(\theta)/R^2, \text{ with } f(\theta=0) = 1 \tag{1}$$

where ρ is the density, A is a constant, and the subscript e refers to the nozzle exit conditions.

3) The inner region is divided into two parts[3]: for small polar angles ($\theta < \theta_o$), the gas originates from the isentropic core of the nozzle, whereas for large polar angles ($\theta > \theta_0$), the gas originates from the nozzle boundary layer. Semiempirical expressions for $f(\theta)$ in both regions have been proposed by Boynton[4] and Simons.[3] Details of the model may be found in Ref. 5. It essentially consists of the model described in Ref. 1, except for some improvements which allow calculations with thick nozzle boundary layers to be made. Thus, the equation

Received Dec. 12, 1975. This work was supported by the Centre National d'Etudes Spatiales.

Index category: Jets, Wakes, and Viscid-Inviscid Flow Interactions.

*Research Associate.

†Research Engineer.

for calculating the constant A becomes

$$A=R_e^2\left[\frac{1}{1+\cos\alpha_e}-\frac{\delta_1}{R_e}+\left(\frac{\delta_1}{R_e}\right)^2\frac{\cos\alpha_e}{2}\right] \Big/ \int_0^{\theta_0}\left[\cos\left(\frac{\pi}{2}\frac{\theta}{\theta_\infty}\right)\right]^{2/(\gamma-1)}\sin\theta\,d\theta \tag{2}$$

The equation for determining θ_0 becomes

$$A=R_e^2\left[\frac{1}{1+\cos\alpha_e}-\frac{\delta}{R_e}+\left(\frac{\delta}{R_e}\right)^2\frac{\cos\alpha_e}{2}\right] \Big/ \int_0^{\theta_0}\left[\cos\left(\frac{\pi}{2}\frac{\theta}{\theta_\infty}\right)\right]^{2/(\gamma-1)}\sin\theta\,d\theta \tag{3}$$

and the relation between the ordinate y in the boundary layer and the polar angle θ becomes

$$\frac{d(y/\delta)}{d\theta}=\frac{-A\sin\theta h(\theta)}{\delta(R_e-y\cos\alpha_e)}\cdot\frac{M_e}{\bar{M}}\cdot\left[\frac{2+(\gamma-1)M_e^2}{2+(\gamma-1)\bar{M}^2}\right]^{1/2} \tag{4}$$

with the same notations as in Ref. 1.

Experiments

Nitrogen jets from small supersonic nozzles exhausted into a still low-density air atmosphere. Thirteen experiments were conducted (runs 1-13). The different parameters (exit Mach number M_e, nozzle half angle α_e, and pressure ratio, P_∞/P_e) were varied independently ($2.28<M_e<6.53$, $0<\alpha_e<30°$, $6.96\times10^{-4}<P_\infty/P_e<2.61\times10^{-2}$). The throat Reynolds number was in the range 1200–23,000, the exit radius R_e was 1.6-5mm, and the boundary-layer thickness in the exit plane was 0.13-0.24 R_e. In each case, the flowfield was investigated using an electron beam probe. The local density was deduced from a photometric measurement of the intensity of the nitrogen first negative system (0-0) band. A correction for nonradiative de-excitation was made. For one of the plumes (run 4), the local rotational temperature T_r also was deduced from the ratio of the intensities of lines 1-2 of the R-branch of the (0-0) band, to the intensity of the whole band. The line intensities were related to the populations of the rotational levels (and thus to T_r) using the Muntz model.[6] The ratio was calculated automatically by means of a ratiometer, allowing on-line measurements of T_r to be made. Details of experimental conditions and results, as well as a more detailed discussion, are given in Ref. 5.

Results and Discussion

Evolution on the Axis

Runs 1 to 4 were carried out by using the same nozzle and the same stagnation conditions P_o, T_o, but the pressure ratio P_∞/P_e was varied. Figure 1 shows the experimental density repartition on the axis of the jets, together with the prediction of the model. X and Z are, respectively, the axial and transverse coordinates. The excellent agreement between theory and experiment confirms: 1) the validity of the source flow assumption (at least near the axis) for abscissa larger than a few exit radii, 2) the fact that the inner part of the jet is unaffected by the external conditions, and 3) the validity of the determination of the constant A, using Eq. (2).

Order of magnitude calculations for rotational and vibrational relaxation led to the conclusion that the vibrational temperature is frozen whereas the rotational temperature is in equilibrium with the translational temperature T. The evolution of T_r on the axis therefore should be deduced from the evolution of ρ by using the isentropic relation, with $\gamma=1.4$. Figure 1 shows that the measured rotational temperature on the axis for run 4 actually agrees with the predicted one within experimental uncertainties.

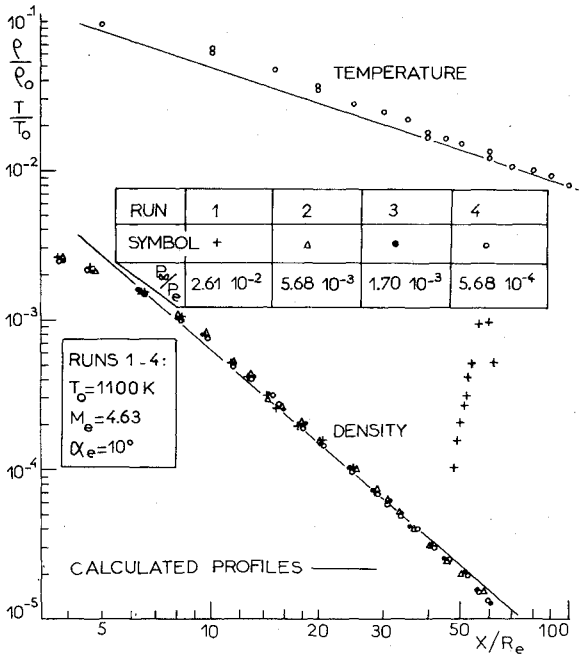

Fig. 1 Axial profiles; temperature and density.

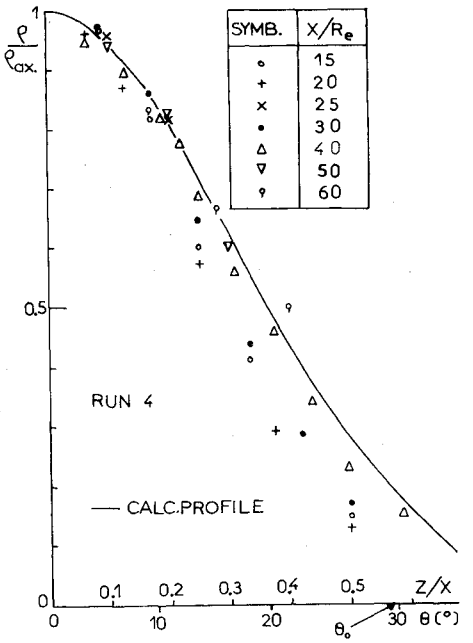

Fig. 2 Transverse profiles; density.

Transverse Profiles

Transverse density profiles for run 4, at various abscissas, have been plotted in Fig. 2, together with the unique profile deduced from the semiempirical expressions of $f(\theta)$ introduced in the model. Both profiles fit together at large abscissas (40-60 R_e), but the calculated one tends to overestimate the density at low abscissas. Perhaps this is because of the failure of the source flow hypothesis at large polar angles and small abscissas. It is nevertheless remarkable that this hypothesis leads to a correct value of A and, consequently, correct values of the density on the axis, even at low abscissas.

The experimental rotational temperature profile and the predicted one for run 4 at the abscissa $X/R_e=10$ have been plotted in Fig. 3. A sudden change in the slope of the predicted temperature profile occurs at $Z/R_e\simeq5.7$, which

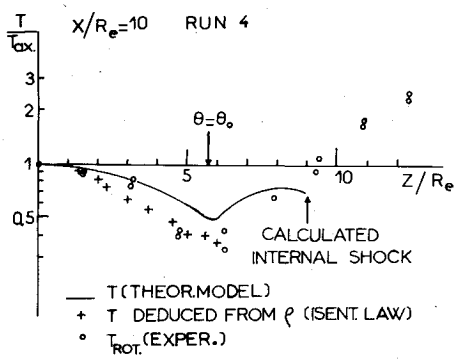

Fig. 3 Transverse profiles; temperature.

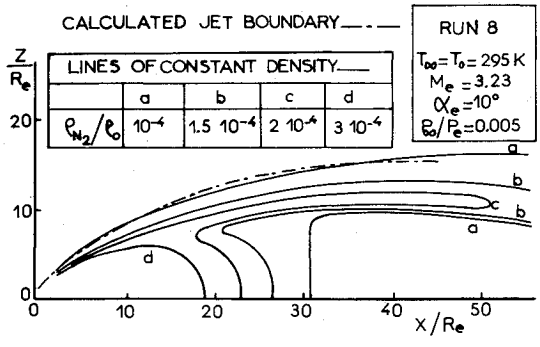

Fig. 4 Jet boundary and lines of constant density.

corresponds to $\theta=\theta_o=29.8°$. This is because of the gradient of static temperature in the exit section of the nozzle, when entering the boundary layer. As the model does not describe the viscous layer, the comparison with the experimental profile must be restricted to the region between the axis and the internal shock. The measured profile exhibits the same overall features as the predicted one. A sudden change in the slope is observed at the predicted value of θ_o, a finding which confirms the validity of the determination of θ_o from Eq. (3), But both profiles really do not coincide. The fact that the measured T_r profile coincides with the T_r profile deduced from the ρ profile, using the isentropic relation, suggests that the discrepancy is mainly because of the inadequacy of the semiempirical $f(\theta)$ at such abscissa, and possibly because of the experimental error.

Jet Boundary

Under our experimental conditions, the gas was so rarefied that the flows could be classified in the transition regime. Diffusion phenomena forbid speaking of a well-defined jet boundary. Draper and Sutton[7] consider that the theoretical boundary obtained from a continuum theory then can be interpreted as the line of equal concentration of the external and the ejected gas, provided that both gases had approximately equal molecular weights. We have plotted in Fig. 4 the lines of equal density deduced from the exploration of the flowfield of run 8, and we developed a very simple calculation for determining the position of the line of equal concentration, based on the following assumption.

Near the boundary, a region exists where the external air diffuses into the ejected nitrogen. We consider this region as a boundary layer with a uniform pressure P_∞, a velocity profile U, and a temperature profile T, related to the U profile by means of the modified Crocco relationship,

$$T=T_\infty+(T_f-T_\infty)\,U/U_L-T_f(U/U_L)^2 \tag{5}$$

where the recovery temperature T_f may be approximated by the local total temperature T_t in the jet at the boundary of the viscous layer. Furthermore, the α profile (concentration of ejected gas) is assumed to coincide with the U profile ($\alpha=U/U_L$). Then, simple calculations lead to

$$\frac{\rho_{N_2}}{\rho_o}=\frac{P_\infty T_o}{P_o T_\infty}\,\frac{\alpha+0.79(1-\alpha)}{1+(T_t/T_\infty-1)\alpha-(T_t/T_\infty)\alpha^2} \tag{6}$$

For run 8, the stagnation temperature T_o is equal to T_∞, so that T_t is approximately equal to T_o all along the boundary. The line of equal concentration $\alpha=½$ coincides with the line of constant density

$$\rho_{N_2}/\rho_o=1.19P_\infty T_o/(P_o T_\infty)=1.16\ 10^{-4} \tag{7}$$

Figure 4 shows that the calculated boundary nearly coincides with the line of equal density $\rho_{N_2}/\rho_o=10^{-4}$. Considering the approximations made in the present calculation, a better agreement was not expected. Nevertheless, it seems that the interpretation by Draper and Sutton for the calculated boundary in the transition regime is confirmed to the present experiment.

References

[1] Lengrand, J. C., "Approximate Calculations of Rocket Plumes with Nozzle Boundary Layers and External Pressure," *Proceedings of the Ninth International Symposium on Rarefied Gas Dynamics*, Vol. 1, Deutsche Forschungs- und Versuchsanstalf für Luft- und Raumfahrt Press, Porz-Wahn, Germany, 1974, B 13.

[2] Albini, F. A., "Approximate Computation of Underexpanded Jet Structure," *AIAA Journal*, Vol. 3, Aug. 1965, pp. 1535-1537.

[3] Simons, G. A., "Effect of Nozzle Boundary Layers on Rocket Exaust Plumes," *AIAA Journal*, Vol. 10, Nov. 1972, pp. 1534-1535.

[4] Boynton, F. P., "Highly Underexpanded Jet Structures. Exact and Approximate Calculations," *AIAA Journal*, Vol. 5, Sept. 1967, pp. 1703-1705.

[5] Lengrand, J. C., "Calculs de Jets Sous-Détendus Issus de Tuyéres Supersoniques," Rapport 75-4, Lab. d'Aérothermique du CNRS, Meudon, France.

[6] Muntz, E. P., "Static Temperature Measurement in a Flowing Gas," *Physics of Fluids*, Vol. 5, Jan. 1962, pp. 80-90.

[7] Draper, J. S. and Sutton, E. A., "A Nomogram for High-Altitude Plume Structures," *Journal of Spacecraft and Rockets*, Vol. 10, Oct. 1973, pp. 682-684.

Hot-Wire and Vorticity Meter Wake Vortex Surveys

A.D. Zalay*
Lockheed Missiles & Space Company, Inc., Huntsville, Ala.

RECENTLTY, as part of a systematic study on wake vortices, surveys have been conducted using both a hot-wire anemometer and a paddle-wheel-type vorticity meter.[1] As anticipated, the hot-wire and vortex meters gave similar results for concentrated trailing vortices. When the vortex wake was "aged" by turbulent injection, however, the vorticity meter significantly underestimated the strength of the vortex field. Comparisons of the vorticity meter and hot-wire wake vortex surveys, summarized briefly in the following Note, indicate that vorticity meters behave in a nonlinear fashion in weak vortex fields.

Measurements have been conducted of the trailing vortex formed 6.5 chord lengths downstream of a 21-in. chord, rec-

Received Nov. 18, 1975; revision received Jan. 30, 1976. Work done under Office of Naval Research sponsorship as an employee of Rochester Applied Science Associates Division of SRL.

Index categories: Aircraft Aerodynamics (including Component Aerodynamics); Aircraft Testing (including Component Wind Tunnel Testing; Jets, Wakes, and Viscid-Inviscid Flow Interactions.

*Senior Research Engineer. Member AIAA.